Turkish Journal of Earth Sciences (Turkish J. Earth Sci.), **Vol. 13**, 2004, pp. 269-286.

Field, Petrographic and Geochemical Characteristics of the Hamit Alkaline Intrusion in the Central Anatolian Crystalline Complex, Turkey

NURDANE İLBEYLİ

Mustafa Kemal University, Tayfur Sökmen Campus, Faculty of Engineering, TR–31040 Hatay – Turkey
(e-mail: ilbeyli@mku.edu.tr)

Abstract: The Hamit pluton is one of the alkaline intrusions in the Central Anatolian Crystalline Complex (CACC). The pluton consists of nepheline syenite, pseudoleucite syenite, alkali-feldspar syenite and quartz syenite. The nepheline syenite and pseudoleucite syenite are cut by foid-bearing microsyenitic dykes, whereas the alkali-feldspar syenite and quartz syenite are cut by aplitic and silicic dykes. The predominantly peralkaline Hamit intrusive rocks possess field, petrographic and geochemical characteristics comparable to A-type granites. All intrusive rocks of this pluton show enrichment in LILE and LREE relative to HFSE. The Th/Yb versus Ta/Yb plot suggests that the intrusive rocks formed from an enriched mantle source region carrying a subduction component inherited from pre-collision subduction events.

Either thermal perturbation of the metasomatised lithosphere by delamination of the thermal boundary layer (TBL) or removal of a subducted plate (slab breakoff) are the likely mechanisms for initiation of the post-collisional magmatism of this complex.

Key Words: Hamit pluton, Central Anatolian Crystalline Complex (CACC), syenite, A-type granites, post-collisional intrusives

Orta Anadolu Kristalen Kompleksi'nde Bulunan Hamit Alkalen İntrüzyonunun Arazi, Petrografik ve Jeokimyasal Özellikleri, Türkiye

Özet: Hamit plütonu, Orta Anadolu Kristalen Kompleksi (OAKK) içerisinde yeralan alkalen intrüzyonlardan biridir. Plüton, nefelin siyenit, psödolösit siyenit, alkali feldspat siyenit ve kuvars siyenitden meydana gelir. Nefelin siyenit ve psödolösit siyenit, foidli mikrosyenitik dayklar tarafından kesilirken, alkali feldspat siyenit ve kuvars siyenit ise aplitik ve silisli dayklar tarafından kesilir. Peralkalen Hamit intrüzif kayaçları arazi, petrografik ve jeokimyasal özellikleri ile A-tipi granitlere benzerlik gösterirler. Tüm intrüzif kayaçlar HFSE nazaran, LILE ve LREE ile zenginleşmiştir. Th/Yb–Ta/Yb diyagramı, intrüzif kayaçlar için kaynak bölgesinin, çarpışma öncesi dalma-batma olayı ile zenginleşmiş manto olduğunu göstermektedir.

Kompleks de çarpışma sonrası magmatizmanın başlangıcı için uygun mekanizmalar, ya metasomatize olmuş litosferin termal sınır tabakasının (TST) delaminasyonu ya da dalmakta olan levhanın (kırılıp?) yok edilmesidir (slab breakoff).

Anahtar Sözcükler: Hamit plüton, Orta Anadolu Kristalen Kompleksi (OAKK), siyenit, A-tipi granitler, çarpışma sonrası granitler

Introduction

Genesis of alkaline magmatism in collision zones (e.g., the Himalayas and Anatolia) has long been the subject of debate, yet their origins remain one of the most interesting and least well understood of all petrological problems. The central Anatolia region exhibits one of the best examples of alkaline magmatism formed in a collision-related tectonic setting. This tectonic region is called the Central Anatolian Crystalline Complex (CACC) and contains Palaeozoic–Mesozoic medium-high grade metamorphic rocks overthrust by Upper Cretaceous ophiolitic units and intruded by a number of calc-alkaline to alkaline plutons (Göncüoğlu *et al.* 1991) (Figure 1). The complex is roughly triangular and surrounded by the İzmir-Ankara-Erzincan Suture Zone to the north, the Tuz Gölü Fault to the southwest and the Ecemiş Fault to the east (Figure 1). Granites and syenites comprise a significant portion of the complex and, thus, have been

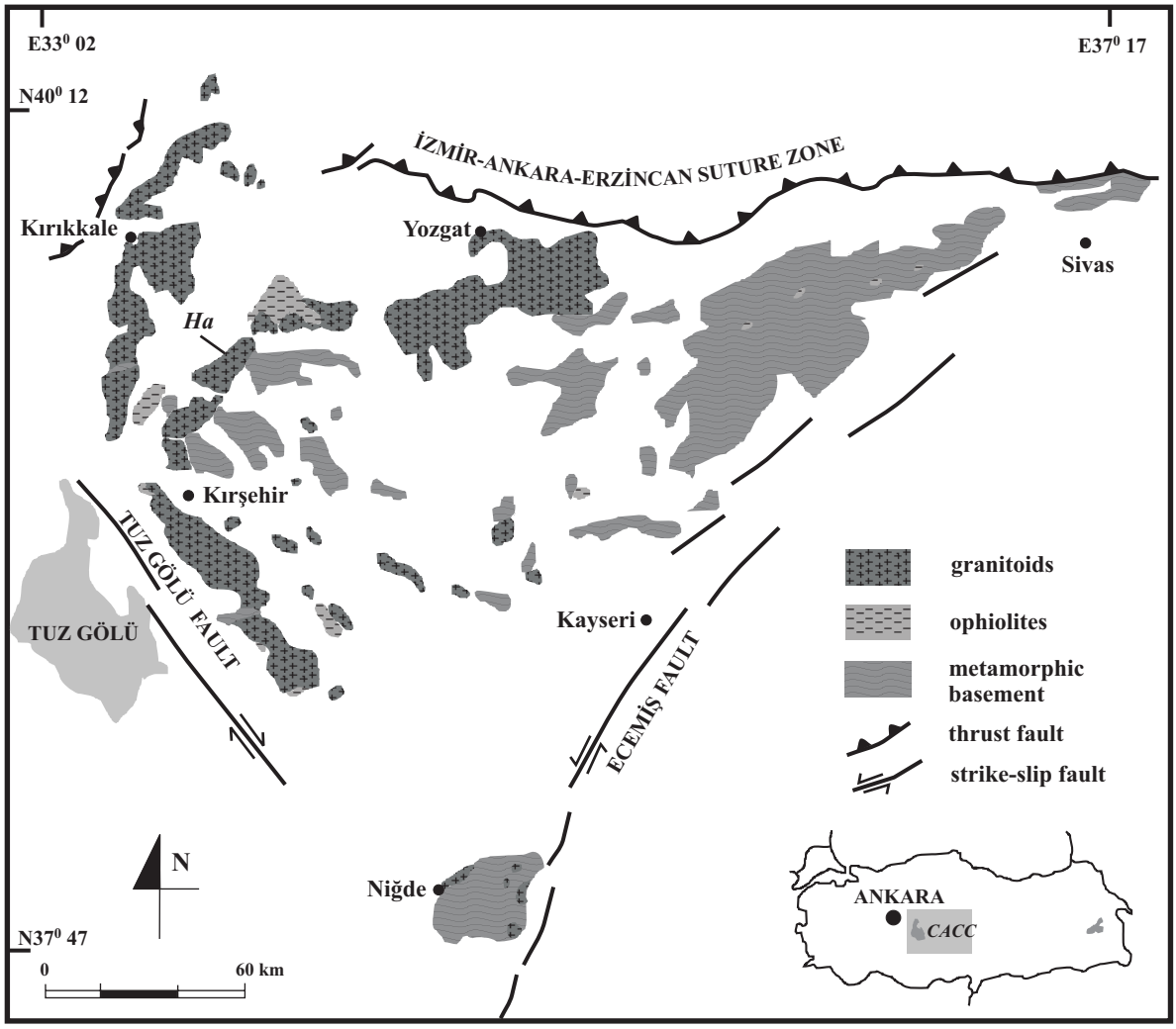

Figure 1. Geological setting of the Central Anatolian Crystalline Complex (CACC) (after Bingöl 1989). Ha– Hamit and CACC– Central Anatolian Crystalline Complex. The inset map shows the complex in relation to the rest of Turkey.

subjected to numerous geological, petrographical and geochemical studies.

Some recent works (e.g., Akıman *et al.* 1993; Ekici *et al.* 1997; Aydın *et al.* 1998, 2001; Boztuğ 1998; Otlu & Boztuğ 1998; İlbeyli 1999; İlbeyli *et al.* 2004) have shown that the magmatic rocks in the complex can be generally divided into four genetically different types: (i) I- (igneous); (ii) S- (sedimentary); (iii) H-(hybrid); and (iv) A- (alkaline).

A number of detailed studies have been carried out on alkaline rocks of the Central Anatolian Crystalline Complex (CACC) (e.g., Lünel & Akıman 1986; Bayhan & Tolluoğlu 1987; Özkan 1987; Tolluoğlu 1993; Boztuğ *et al.* 1994; Özkan & Erkan 1994; Göncüoğlu *et al.* 1993, 1997; Boztuğ 1998, 2000; Otlu & Boztuğ 1998; İlbeyli 1999; Köksal *et al.* 2001), but the geneses of these rocks are still a subject of debate.

For the origin of the A-type granites in the Central Anatolian Crystalline Complex (CACC), several theories have been set forth. For example, Lünel & Akıman (1986) studied the alkaline rocks in the Hamitköy area. They suggested that the syenitic batholith is cut by microsyenitic dykes. The presence of pseudoleucites as feldspathoids in the dykes indicates that the source magma was silica-poor and volatile-rich (Lünel & Akıman 1986). Özkan (1987) studied the alkaline rocks in the

Hayriye (Kayseri) region, suggesting that the Atdere foid syenite may have formed by partial melting of the residue after the formation of I-type granitoids. In a complementary work, Özkan & Erkan (1994) pointed out that the foid syenite was derived from an undersaturated potassic melt fractionated towards a Na-rich sodalite-nepheline syenite. Bayhan & Tolluoğlu (1987) determined that the Çayağazı syenitoid to the northwest of Kırşehir comprises microcline syenites, felsic dykes and nepheline-bearing syenites, and suggested that these rocks formed by partial melting of different sources. Bayhan (1988) noted the syenitoids in the Bayındır-Akpınar area and suggested that they formed from discrete magma sources and were not fractionated from a single parental magma. Tolluoğlu (1993) examined the Buzlukdağ syenitoid and the Kötüdağ Volcanite in the CACC. He demonstrated that the Buzlukdağ Syenitoid is alkaline in character, containing quartz syenite, syenite and monzonite. However, the Kötüdağ volcanite is calc-alkaline to alkaline, comprising rhyolite, dacite, trachyte and trachyandesite/andesite. Thus, the Buzlukdağ syenitoid and the Kötüdağ volcanite formed from different magma sources (Tolluoğlu 1993). Göncüoğlu *et al.* (1993) notified that the syenitoids in the CACC are of lower crust-upper mantle origin and are post-collisional intrusions of Early Maastrichtian age. Boztuğ *et al.* (1994) suggested that the alkaline rocks in the CACC were derived from an upper-mantle source during extensional event in the passive margin towards the final stages of crustal thickening. Crustal contamination was also operative in their genesis (Boztuğ *et al.* 1994). According to Göncüoğlu *et al.* (1997), the İdiş Dağı syenitoids are a late-stage member of the central Anatolian plutonics, formed by crustal anatexis. Boztuğ (1998) suggested that the alkaline plutons constitute an important association in the post-collisional central Anatolian granitoids. The magma source of this plutonism can be derived by partial melting of an upper mantle source (Boztuğ 1998). Otlu (1998) and Otlu & Boztuğ (1998) studied the Kortundağ and Baranadağ plutons and suggested that the alkaline rocks in the region can be subdivided into two subgroups: (i) silica-oversaturated alkaline (ALKOS) and (ii) silica-undersaturated alkaline (ALKUS). The latter occur as dykes cutting the former. Otlu & Boztuğ (1998) pointed out that these plutons were probably derived from two different alkaline magmas. These magmas could have been derived by partial melting of upper-mantle source rocks due to adiabatic decompression under a tensional regime after crustal thickening following the Anatolide-Pontide collision (Otlu & Boztuğ 1998). Köksal *et al.* (2001) suggested that the syenitoid rocks are the final phase of magmatism in the CACC. Their chemical features point towards a largely mantle-derived magma contribution together with a noticeable crustal component in their genesis (Köksal *et al.* 2001). The syenitoid rocks formed during post-collisional uplift that followed crustal thickening related to southward emplacement of ophiolitic nappes during closure of the İzmir-Ankara-Erzincan ocean strand of Neo-Tethys (Köksal *et al.* 2001).

Since there is an on-going debate about the origin of the A-type granites in the CACC, this paper is concerned only with A-type intrusives in the complex. Here, I present new major- and trace-element (including REEs) data for well-characterised samples from the A-type plutons emplaced at the western edge of the complex. These geochemical data might shed light on the genesis of alkaline intrusives in a post-collisional tectonic setting.

Geological Setting

Turkey is situated on an important component of the Alpine-Himalayan orogenic system. Its structure comprises a number of continental blocks separated by ophiolitic suture zones (Figure 1); this complex structure developed as a result of closure of the different branches of the Neo-Tethyan Ocean during the Late Cretaceous–Eocene (Şengör & Yılmaz 1981). According to Şengör & Yılmaz (1981), the closure of Palaeo-Tethys during the Middle Jurassic meant that only two oceans were left in Turkey: the multi-branched northern and the relatively simpler southern branches of Neo-Tethys. Şengör & Yılmaz (1981) postulated that the northern branches of Neo-Tethys consisted of the İzmir-Ankara-Erzincan and the Inner Tauride oceans and, that these together with the Bitlis-Pötürge fragment, separated the Anatolide-Tauride Platform from Eurasia; the southern branch separated the platform and fragment from the main body of Gondwanaland. On the basis of Şengör & Yılmaz's (1981) model, the Intra-Pontide and the İzmir-Ankara-Erzincan oceans isolated the Sakarya Continent within the northern branches of Neo-Tethys. The İzmir-Ankara-Erzincan ocean began opening between the Sakarya Continent to the north and the Anatolide-Tauride

Platform to the south during the Early Jurassic (Lias) (Görür *et al.* 1984). This ocean reached its maximum size during the Early Cretaceous (Şengör & Yılmaz 1981) and started to close at the beginning of the Late Cretaceous along two north-dipping subduction zones beneath the Pontides (Tüysüz *et al.* 1995). Subsequently, ophiolite and ophiolitic mélange slivers from the İzmir-Ankara-Erzincan ocean were obducted southwards onto the northern margin of the Anatolide-Tauride Platform. This obduction caused crustal thickening, metamorphism and subsequent granite plutonism at the northern edge of the platform. The Anatolide-Tauride Platform and the Pontides subsequently collided during the Late Palaeocene–Eocene (Şengör & Yılmaz 1981).

The continental collisions in Turkey mainly took place in two episodes: (i) the more recent, and better known, Eocene continent-Pontide arc collision; and (ii) the earlier Cretaceous continent-island arc collision that predated the Pontides (e.g., Okay *et al.* 2001) and is the subject of this study. Plutons of latest Cretaceous age throughout the Central Anatolian Crystalline Complex (CACC) are one of the major indicators of this latter collision.

Within the complex, three main lithological associations make up the metamorphic basement into which the intrusives were emplaced. Seymen (1981, 1982) summarised these associations, as follows: (i) the Kalkanlıdağ formation, which is characterised by a complex of gneisses, biotite schists, pyroxene schists, quartzites, quartz schists and calc-silicate schists; (ii) the Tamadağ formation, which is an intercalation of marbles, schists and gneisses; and (iii) the Bozçaldağ formation, which is composed primarily of marbles, metachert-bearing marbles and metacherts. Seymen (1985) also mentioned that there is no direct evidence either for the age of the protoliths or for the age of the metamorphic rocks, although the unconformably overlying non-metamorphic Late Maastrichtian clastics define the upper age limit.

The crystallisation ages for the central Anatolian intrusives are also still debated. Previous age determinations (whole-rock Rb-Sr / mineral K-Ar) on different intrusives in the complex include the following: 71±1 Ma (Cefalıkdağ granodiorite: Ataman 1972), 95±11 Ma (Üçkapılı granodiorite: Göncüoğlu 1986), 110±5 Ma (Murmano pluton: Zeck & Ünlü 1987), 70.7±1.1 Ma (Bayındır syenitoid: Gündoğdu *et al.* 1988), 85.1±3.6 Ma (Bayındır syenitoid: Kuruç 1990), 110±14 Ma (Ağaçören granitoid: Güleç 1994), 67.1±1.3 Ma (Terlemez quartz monzonite: Yalınız *et al.* 1998), 79.5±1.7, 66.6±1.1, 76.4±1.3 Ma (Behrekdağ granite, Cefalıkdağ quartz monzonite, Baranadağ monzonite: İlbeyli 1999; İlbeyli *et al.* 2004) and 77.7±0.3 Ma (Ağaçören granite: Kadıoğlu *et al.* 2003).

Intrusive Petrology

The Hamit pluton was defined as a part of the Buzlukdağ pluton by Seymen (1982), but was described as a separate unit by Erler *et al.* (1991). This pluton has also been named as a part of the Kortundağ pluton (Otlu 1998; Otlu & Boztuğ 1998). The Hamit pluton crops out to the northeast of Kaman, covering an area of about 120 km^2, and is bounded by the Kaman group, the Karakaya ultramafic rocks and cover units (Figure 2).

The Hamit pluton is composed of foid monzosyenite (nepheline monzosyenite, pseudoleucite monzosyenite), alkali-feldspar syenite and quartz syenite (Figure 3, Table 1). In the field, these rock types are distinguished from one another mainly on the basis of their colour and the composition of their megacrysts. The nepheline monzosyenite is dark grey-green, medium-grained, occasionally porphyritic with alkali-feldspar megacrysts (up to 5 cm across). The pseudoleucite monzosyenite is grey-dark grey and porphyritic with prismatic alkali-feldspar and euhedral pseudoleucite megacrysts (up to 8 cm across). The alkali feldspar syenite is pink and medium-grained. The quartz syenite is cream-coloured, medium-grained and variably porphyritic with prismatic alkali feldspar (up to 4 cm across). The nepheline monzosyenite and pseudoleucite monzosyenite tend to crop out in the central part of the pluton, whereas the quartz syenite roughly makes up the rim of the pluton, with the alkali-feldspar syenite between them. The alkali-feldspar syenite and quartz syenite are cut by aplitic and silicic dykes. The nepheline monzosyenite and pseudoleucite monzosyenite are cut by foid-bearing microsyenitic dykes.

The nepheline monzosyenite is medium-grained with a hypidiomorphic, granular texture (Figure 4). It contains a greater proportion of mafic minerals (~%70) than the alkali-feldspar syenite and quartz syenite. Microperthitic alkali feldspar is the dominant mineral in the nepheline monzosyenite. The interstices between other crystals in this lithology are generally filled by nepheline. Plagioclase feldspar (An_{49-24}, Table 2) is euhedral to subhedral and

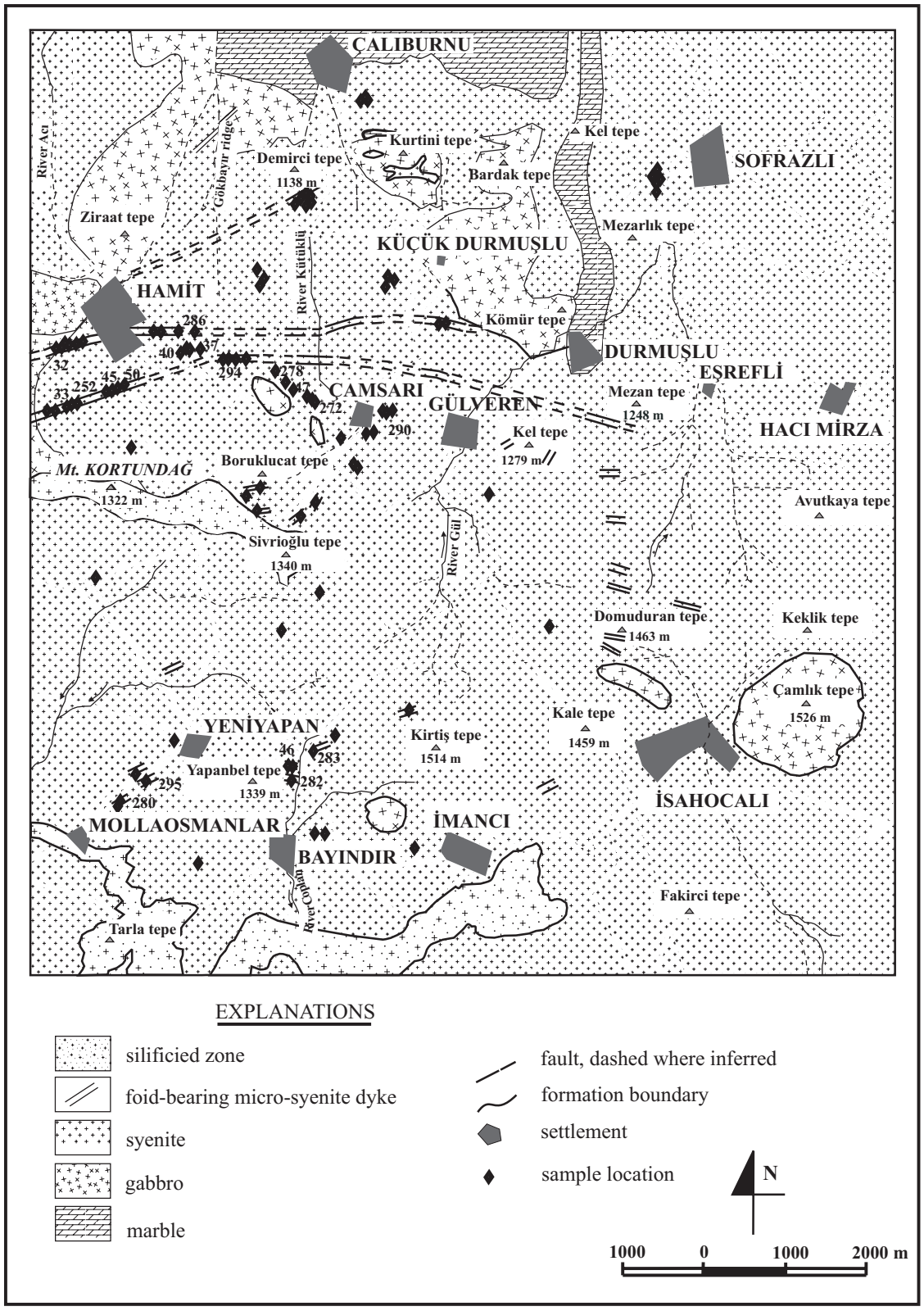

Figure 2. 1/25,000 scale geological map of the Hamit pluton (after Dalkılıç 1986 and references therein).

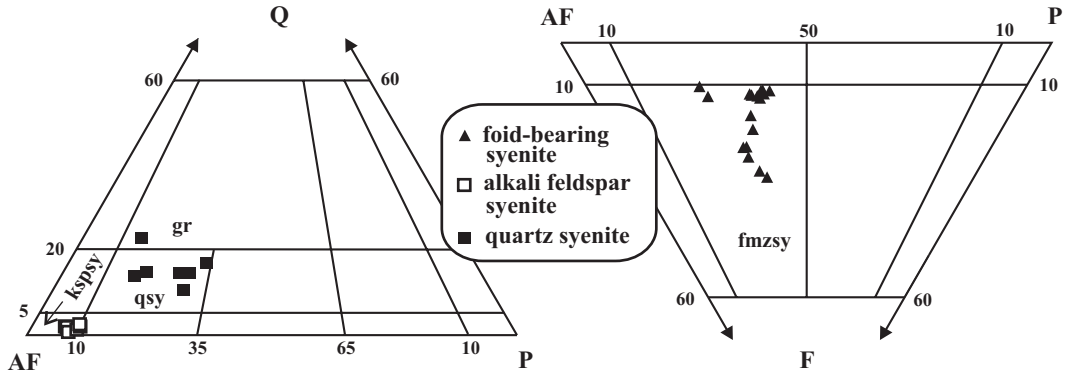

Figure 3. Quartz-alkali feldspar-plagioclase-foid (QAPF) modal mineralogy of the Hamit intrusives, based on a minimum 1200 points per thin sections. Classification of granitic rocks from Streckeisen (1976). gr– granite, qsy– quartz syenite, kspsy– alkali-feldspar syenite and fmzsy– foid monzosyenite.

Table 1. Representative modal analyses of the Hamit intrusives. Values are in percent. tr– trace.

Sample no	N45 *	N294 *	N50 *	N295 *	N283 *	N282 *	N280 *	N37	N40	N47	N290	N265
Nepheline	14.4	13.0	10.3	14.2	8.6	10.1	9.7					
Alkali feldspar	43.0	42.1	43.0	36.0	42.4	47.8	42.7	1.2	1.8	15.9	14.0	23.0
Plagioclase	21.0	21.0	27.2	20.3	27.2	28.0	26.5	87.8	86.6	49.8	56.8	65.0
Clinopyroxene	9.3	6.1	8.3	8.6	10.2	8.0	11.3	9.3	9.6	26.2	22.4	11.6
Amphibole	1.3	0.2	1.2	2.1	6.4	3.3	5.6	1.0	1.7	7.8	4.7	-
Biotite	0.1	tr	tr	tr	0.2	1.2	0.1	0.2	0.1	0.1	tr	0.3
Pseudoleucite	5.0	6.6	-	7.8	-	-	-	0.1	tr	-	1.2	-
Nosean	0.8	3.4	-	2.2	-	-	-	0.1	tr	0.1	0.4	0.1
Garnet	3.4	4.2	6.5	5.6	-	-	-	0.1	-	0.1	-	-
Cancrinite	1.2	3.0	3.2	2.8	4.5	1.4	3.7	tr	-	-	-	-
Titanite	0.1	tr	0.1	0.1	0.2	0.1	0.1	0.1	0.1	-	-	-
Apatite	0.1	0.1	0.1	tr	0.1	tr	0.2	0.1	0.1	0.1	0.4	0.1
Opaques	0.3	0.2	0.1	0.2	0.1	0.1	0.2					

**Fluorite: all samples*
**Zircon: all samples*

normally zoned. Clinopyroxene (salite), amphibole (hastingsite) (İlbeyli 1999) and biotite are the mafic minerals. Accessory minerals are titanite, apatite, zircon, fluorite and opaques. Garnet has also been observed as euhedral crystals and is zoned. The most common alteration product is cancrinite after nepheline.

The pseudoleucite monzosyenite is porphyritic with hypidiomorphic, granular texture. Phenocrysts are pseudoleucite, plagioclase (An_{71-48}), alkali feldspar, clinopyroxene (salite) (Figure 4) (İlbeyli 1999) and, occasionally, amphibole (hastingsite) and garnet. The matrix is fine- to medium-grained containing nepheline, nosean, garnet and plagioclase feldspar. Accessory minerals are titanite, apatite, opaques, zircon and fluorite. Pseudoleucite has resulted from an intergrowth of nepheline and alkali feldspar and has well-defined boundaries. Cancrinite is the most common secondary mineral after nepheline.

The alkali-feldspar syenite is medium-grained, equigranular with hypidiomorphic, granular texture (Figure 5). The dominant mineral is microperthitic alkali feldspar, which occurs as tabular, euhedral to subhedral crystals, and comprises up to 90% of the rock by volume. Plagioclase feldspar (An_{9-1}) is euhedral to subhedral and forms about 10% of the rock. Accessory minerals are quartz, amphibole, clinopyroxene, biotite, titanite,

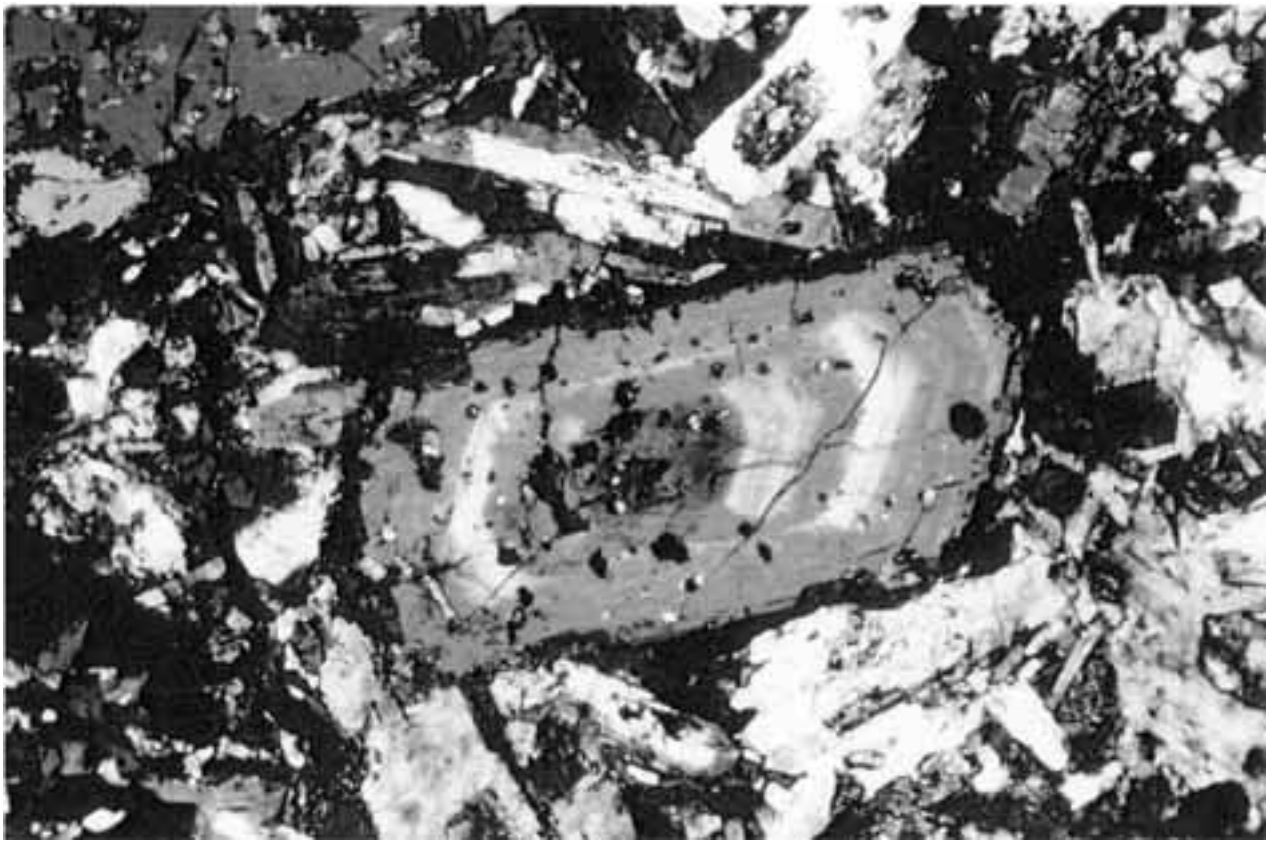

Figure 4. Photomicrograph of nepheline monzosyenite (sample N32) from the Hamit pluton with a zoned prismatic clinopyroxene. The remaining minerals seen in the view are alkali feldspar, nepheline and plagioclase feldspars. Magnification: 3x1.9 mm, XPL.

opaques, apatite, zircon and allanite. Muscovite and epidote occur as alteration products after feldspar.

The quartz syenite has characteristics similar to the alkali-feldspar syenite but with higher proportions of quartz and mafic minerals. The microperthitic alkali feldspar occurs as prismatic and euhedral to subhedral crystals. Its microperthitic texture is not as well-developed as in the alkali-feldspar syenite. Plagioclase feldspar (An_{20-1}) is euhedral to subhedral and exhibits complex oscillatory zoning. Quartz is interstitial. Amphibole (edenite), clinopyroxene (salite) (İlbeyli 1999) and biotite are occur as mafic minerals. Accessory minerals are titanite, opaque phases, apatite and zircon. Sericite occurs as a secondary mineral after feldspars.

Analytical Techniques

A number of representative fresh samples were powdered using an agate ball mill. Major elements were analysed on fused glass discs and trace elements on pressed powder pellets by X-ray fluorescence spectrometry (XRF) at the University of Durham (U.K.) using an automated Philips PW 1400 spectrometer with an Rh anode tube. Loss on ignition (L.O.I) was determined by heating a separate aliquot of rock powder at 900 °C for >2 h. Analyses of the REEs and a number of other elements (e.g., Hf, Ta, Th, Pb, U) were determined by acid ($HF-HNO_3$) digestion of fused glass discs rather than powders to ensure dissolution, followed by analyses at the University of Durham by inductively coupled plasma-mass spectrometry (ICP-MS). Errors and analytical precision are given in Peate *et al.* (1997). The full data set is presented in Table 3.

Geochemistry

Whole-rock major- and trace-element analyses of the representative Hamit samples are given in Table 3. The intrusive rocks from the pluton have a range of silica contents, from approximately 53 to 72 wt%, and are

Table 2. Representative mineral analyses of the Hamit intrusive rocks. Structural formulae of the clinopyroxenes on the basis of 6 O, of the amphiboles are on 23 O, and of the feldspars are on 8 O. pdsy– pseudoleucite monzosyenite, nesy– nepheline monzosyenite, kspsy– alkali feldspar syenite, qsy– quartz syenite, cpx– clinopyroxene, amp– amphibole and felds– feldspar.

Sample no	N46	N32	N294	N50	N32	N278	N290	N46	N32	N50	N272	N290
Rock composition	pdsy	nesy	pdsy	nesy	nesy	kspsy	qsy	pdsy	nesy	nesy	kspsy	qsy
Mineral	*cpx*	*cpx*	*cpx*	*cpx*	*amp*	*amp*	*amp*	*felds*	*felds*	*felds*	*felds*	*felds*
SiO_2	43.37	48.74	42.95	41.07	36.48	36.42	43.16	64.73	62.08	54.89	64.84	68.34
TiO_2	1.69	1.01	1.64	1.69	1.72	1.40	0.78	0.05	0.00	0.04	0.00	0.00
Al_2O_3	7.24	4.37	7.10	8.11	13.27	12.01	7.94	18.82	23.39	27.47	18.31	19.51
Cr_2O_3	0.02	0.01	0.01	0.00	0.00	0.03	0.01	0.01	0.01	0.00	0.01	0.02
FeO	15.14	8.95	15.92	19.55	21.82	24.30	16.88	0.21	0.07	0.56	0.05	0.17
MnO	0.40	0.34	0.39	0.65	0.62	1.54	1.18	0.00	0.00	0.02	0.01	0.00
MgO	8.02	12.62	7.70	4.88	6.52	4.65	10.92	0.01	0.01	0.02	0.01	0.02
CaO	22.76	22.47	22.68	22.08	11.28	11.01	11.57	0.60	5.15	10.08	0.02	0.29
BaO	0.03	0.03	0.00	0.06	0.01	0.06	0.04	0.00	0.03	0.01	0.08	0.02
Na_2O	0.79	0.73	0.78	1.08	2.41	2.53	2.32	2.59	8.64	5.08	0.58	11.50
K_2O	0.02	0.00	0.00	0.01	2.23	2.07	1.29	12.43	0.27	1.08	15.56	0.12
TOTAL	99.48	99.27	99.17	99.18	96.36	96.02	96.09	99.45	99.65	99.25	99.47	99.98
Si	1.679	1.834	1.673	1.628	5.853	5.968	6.688	2.975	2.764	2.502	3.004	2.989
Ti	0.049	0.029	0.048	0.051	0.208	0.173	0.091	0.002	0.000	0.001	0.000	0.000
Al	0.330	0.194	0.326	0.379	2.510	2.320	1.451	1.019	1.228	1.476	1.000	1.006
Cr	0.001	0.000	0.000	0.000	0.000	0.004	0.001	0.000	0.000	0.000	0.000	0.001
Fe	0.460	0.267	0.486	0.610	2.928	3.330	2.188	0.008	0.003	0.019	0.002	0.006
Mn	0.013	0.011	0.013	0.022	0.084	0.213	0.155	0.000	0.000	0.001	0.000	0.000
Mg	0.463	0.708	0.447	0.289	1.559	1.135	2.523	0.000	0.000	0.001	0.001	0.001
Ca	0.944	0.906	0.947	0.938	1.939	1.933	1.920	0.030	0.246	0.492	0.001	0.013
Ba	0.001	0.001	0.000	0.001	0.000	0.004	0.002	0.000	0.000	0.000	0.001	0.000
Na	0.059	0.053	0.059	0.083	0.749	0.804	0.698	0.230	0.746	0.449	0.052	0.975
K	0.001	0.000	0.000	0.001	0.457	0.434	0.256	0.728	0.015	0.063	0.919	0.007
TOTAL	4.000	4.003	3.999	4.002	16.287	16.318	15.973	4.992	5.002	5.004	4.980	4.998
Wollastonite	50.23	47.91	50.03	50.49			Albite	23.30	74.10	44.70	5.40	98.00
Enstatite	24.62	37.42	23.62	15.52			Orthoclase	73.70	1.50	6.30	94.50	0.70
Ferrosilite	25.16	14.67	26.35	33.99			Anorthite	3.00	24.40	49.00	0.10	1.30

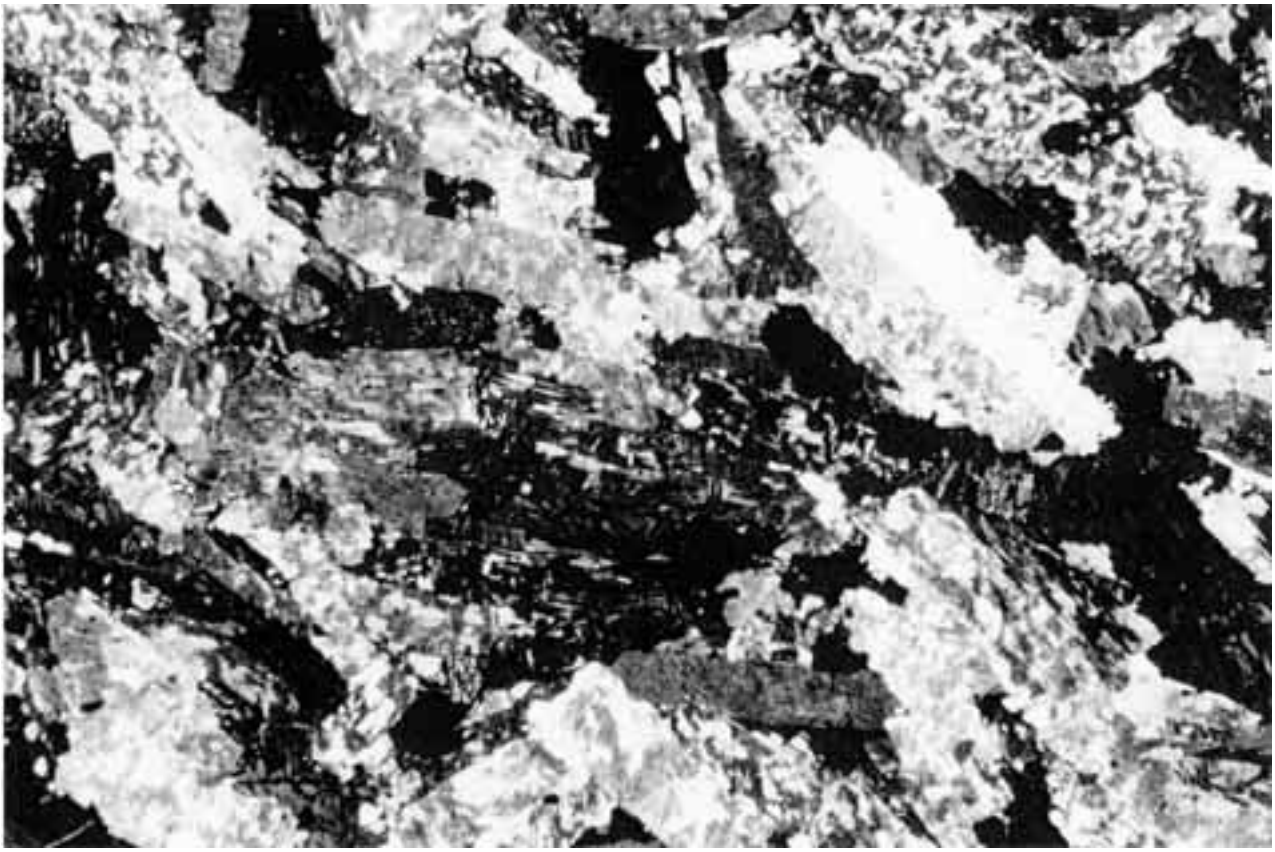

Figure 5. Photomicrograph of tabular alkali feldspars in the alkali-feldspar syenite (sample N40) show strong microperthitic texture. Alkali feldspars also display typical simple twinning. Magnification: 6x3.7 mm, XPL.

plotted on Figure 6 with silica as the index of differentiation. As can be seen from Figure 6, samples from this pluton lie in negatively correlated linear arrays on Harker variation diagrams for TiO_2 and CaO. However, Al_2O_3 has two distinct ranges for the Hamit rocks: (i) Al_2O_3 increases steadily for the foid-bearing rocks (nepheline monzosyenite and pseudoleucite monzosyenite) and (ii) decreases for the alkali-feldspar syenite and quartz syenite. P_2O_5 also has two distinct ranges for the intrusive rocks: (i) P_2O_5 decreases for the foid-bearing rocks (nepheline monzosyenite and pseudoleucite monzosyenite) and (ii) increases for the alkali-feldspar syenite and quartz syenite.

The Hamit intrusive rocks have been classified chemically using the total alkali versus silica diagram of Irvine & Baragar (1971) (Figure 7a). As can be seen from this diagram, the intrusive rocks of the Hamit pluton plot in the alkaline field. On the basis of the alumina saturation diagram of Shand (1951) (Figure 7b), the foid-bearing rocks are metaluminous, whereas the alkali-feldspar syenite and quartz syenite are peralkaline.

The rocks from the Hamit pluton show LREE enrichment (La_N/Yb_N=27.44–56.10 for the least acidic and 22.61–41.68 for the most acidic samples) with small to moderate negative Eu anomalies (Eu/Eu*=0.68–0.85 for the former and 0.58–0.67 for the latter) (Figure 8). The Hamit intrusive rocks have LREE/MREE ratios of 8.19–14.48 for the least acidic and 19.66–33.56 for the most acidic samples, and MREE/HREE ratios of 3.27–3.87 for the former and 1.15–3.12 for the latter.

Representative intrusive rock samples (quartz syenite samples > 5% of modal quartz) from the pluton were normalised to the hypothetical ocean ridge granite (ORG) (Pearce *et al.* 1984) (Figure 9). All samples are characterised by enrichments in LILE (K, Rb, except Ba reflecting dominant control of alkali feldspar) and LREE (Ce, Sm) relative to HFSE (Ta, Nb, Hf, Zr, Y and Yb). In addition, they have low values of Y and Yb relative to the normalising compositions.

Table 3. XRF-major element (wt%) and trace element (ppm) analyses of the representative samples from the Hamit intrusion. pdsy– pseudoleucite monzosyenite, nesy– nepheline monzosyenite, pho– phonolite, kspsy– alkali feldspar syenite, qsy– quartz syenite.

Sample no	N45	N33	N252	N294	N286	N285	N50	N278	N37	N40	N272	N47	N490
Rock type	*pdsy*	*nesy*	*nesy*	*pdsy*	*pho*	*nesy*	*pdsy*	*kspsy*	*kspsy*	*kspsy*	*qsy*	*qsy*	*metasediment*
SiO_2	52.83	53.32	53.58	54.23	55.94	56.09	56.45	60.96	62.23	64.72	65.06	65.88	74.96
TiO_2	0.62	0.72	0.74	0.62	0.20	0.51	0.43	0.41	0.35	0.32	0.28	0.30	0.17
Al_2O_3	19.15	18.09	18.36	18.98	22.83	20.42	20.07	18.73	19.01	18.16	18.96	17.29	12.52
Fe_2O_3 tot	5.39	6.49	6.49	5.19	2.20	4.44	3.72	2.91	2.43	1.72	0.79	2.16	1.61
MnO	0.14	0.15	0.14	0.13	0.14	0.12	0.12	0.13	0.08	0.02	0.04	0.07	0.02
MgO	1.47	2.97	3.02	1.40	0.06	1.08	0.53	0.29	0.15	0.04	0.08	0.42	0.71
CaO	6.72	7.01	6.98	6.93	2.03	3.59	4.93	2.55	1.93	0.91	0.65	1.84	1.57
Na_2O	4.29	3.37	3.35	3.76	7.92	4.93	4.87	3.92	4.51	4.95	4.30	4.29	2.14
K_2O	7.87	6.71	6.67	7.83	8.08	7.99	8.47	9.01	8.32	8.29	9.86	6.98	5.58
P_2O_5	0.31	0.42	0.41	0.31	0.02	0.25	0.11	0.03	0.04	0.05	0.02	0.05	0.03
L.O.I	1.43	1.05	1.49	2.12	3.12	0.77	1.81	0.66	0.38	0.62	0.66	0.31	1.12
TOTAL	98.78	99.25	99.73	99.38	99.42	99.42	99.70	98.93	99.04	99.18	100.04	99.27	99.32
Sc	10	8	7	7		3	6	4	3			4	5
Cr	1	40	24	3	21	21	2	2		29		12	5
V	97	123	121	75	32	52	49	46	38	33	11	25	19
Ni	13	15	32	14	13	5	9			6	9	6	2
Co	10	13	13	9	2	7	4	2	4				1
Cu	6	34	28	32	1	25		12	9	1	3	1	20
Zn	93	108	89	86	104	96	91	62	44	58	27	41	12
Ga	17	26	23	18	27	20	17	12	18	20	14	21	12
Rb	264	226	216	273	350	256	290	284	260	480	370	350	262
Sr	1260	1294	1073	1369	153	1391	1453	190	196	104	162	270	85
Y	45	40	42	49	43	33	30	79	38	45	28	37	21
Zr	436	369	351	403	809	375	424	270	117	279	92	317	124
Nb	45	28	31	38	73	35	38	45	38	38	42	20	14
Ba	949	1248	1493	2082	71	1345	1470	32	41	22	149	295	662
La	122.09	112.68	116.51	92.40	149.24	103.84	130.57	102.07	121.46	138.95	74.64	140.71	38.59
Ce	223.53	208.86	171.51	172.00	216.60	160.73	192.88	168.58	202.95	189.29	130.91	187.78	67.59
Pr	24.24	23.03	23.22	20.54	22.29	19.71	23.47	21.31	20.10	23.83	13.30	18.44	8.06
Nd	86.42	76.77	83.44	73.54	59.99	66.56	75.61	73.44	57.67	67.33	38.82	50.72	30.43
Sm	13.77	13.57	13.67	11.90	6.79	10.00	10.11	12.61	8.50	8.77	4.71	6.24	5.20
Eu	2.88	2.89	2.96	2.67	0.92	2.27	2.14	2.20	1.47	1.36	0.79	0.99	0.85
Gd	12.00	9.58	9.91	8.35	4.12	6.72	6.23	10.21	5.49	5.79	2.75	4.18	4.38
Tb	1.25	1.00	1.24	1.08	0.59	0.86	0.79	1.66	0.73	0.83	0.39	0.63	0.64
Dy	6.00	5.16	5.87	5.35	2.94	4.12	3.69	9.80	4.44	4.26	1.87	3.25	3.53
Ho	1.04	0.83	1.03	0.93	0.58	0.74	0.65	2.15	0.85	0.81	0.33	0.65	0.71
Er	2.77	2.14	2.61	2.45	1.74	1.94	1.66	6.87	2.63	2.27	0.86	1.97	1.84
Tm	0.43	0.32	0.41	0.39	0.32	0.31	0.26	1.28	0.46	0.38	0.13	0.36	0.31
Yb	2.50	2.25	2.41	2.27	2.19	1.92	1.57	8.56	3.62	2.25	0.72	2.39	1.92
Lu	0.37	0.32	0.37	0.34	0.35	0.29	0.23	1.37	0.52	0.33	0.10	0.39	0.31
Hf	8.25	7.32	8.26	8.33	13.56	7.39	8.43	6.78	2.99	5.41	2.75	8.61	3.61
Ta	3.09	2.13	2.22	2.89	3.02	2.62	2.64	2.78	2.50	2.93	2.71	1.97	0.42
Pb	63.05	51.51	55.45	69.30	129.32	72.67	94.24	66.03	47.24	69.81	68.46	67.05	52.49
Th	59.89	50.91	51.77	28.46	130.12	62.00	60.99	71.07	72.01	143.30	53.83	137.09	18.43
U	18.46	13.72	11.75	19.26	46.19	18.15	20.95	13.85	5.76	17.72	6.60	18.08	4.84

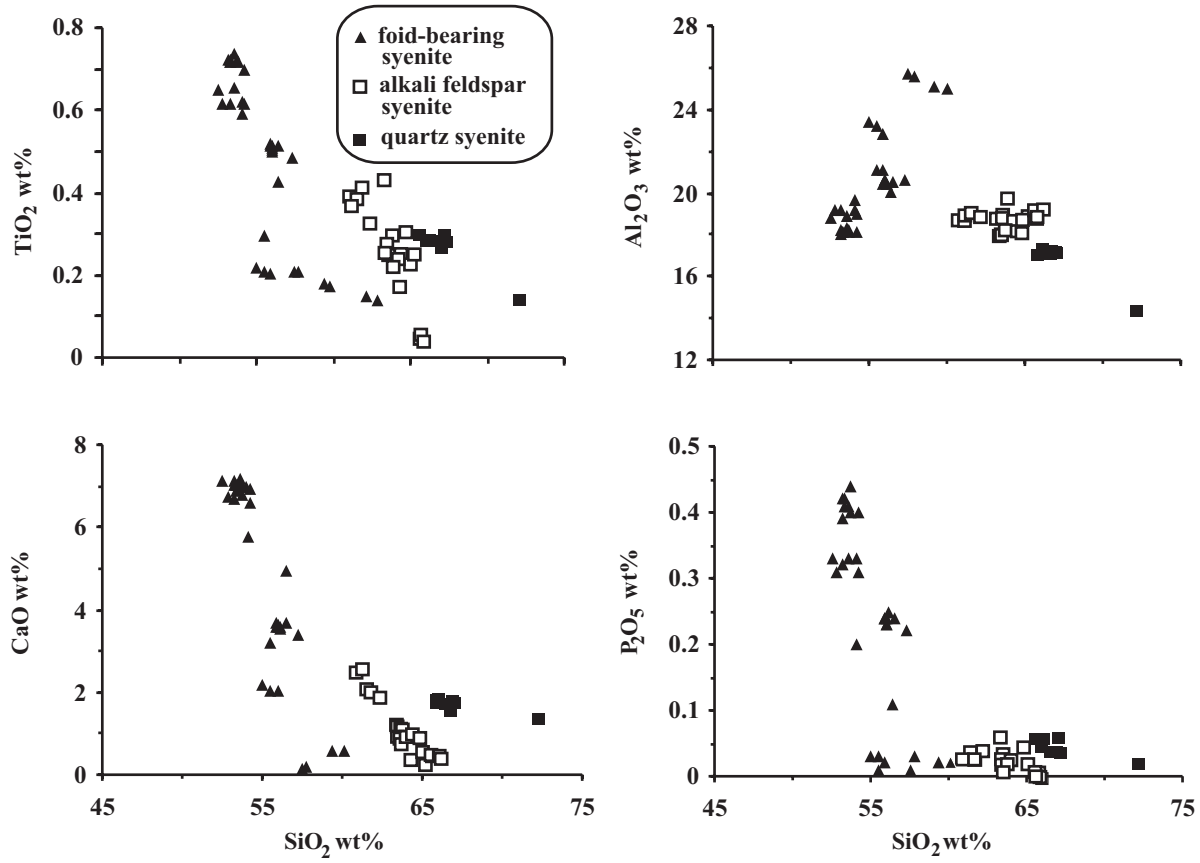

Figure 6. Selected major-element variation diagrams for the Hamit intrusives.

When samples from the Hamit pluton are plotted on the tectonic discrimination diagrams of Pearce *et al.* (1984), the Hamit rocks fall into the within-plate granite (WPG) field in the Nb versus Y diagram (Figure 10a), consistent with the alkaline character of the intrusion. In the Rb against (Y+Nb) discrimination diagram (Figure 10b), most of the Hamit intrusive samples plot within the post-COLG field as described by Pearce *et al.* (1984) and Pearce (1996). It is possible that mobility of Rb in Figure 10b could result in a shift from the WPG field to the syn-COLG field.

Discussion and Conclusions

The genesis of A-type (alkaline) granites has been the subject of much research. Some workers have argued that A-type granites are generated through partial melting of the lower crust (e.g., Duchesne 1984, 1990; Huppert & Sparks 1988; Emsile & Stirling 1993), while others have inferred that there are genetic links between mantle-derived melts and A-type granites (e.g., Turner *et al.* 1992).

The best model for the origin of the alkaline plutonic rocks should explain the coexistence of silica-undersaturated (the foid-bearing) and silica-saturated (the alkali feldspar/quartz syenite) magmatism at the same time in the same tectonic setting. The primary composition of source material, the role of water, and the type and degree of partial melting processes may also play an important part in the genesis and evolution of an alkaline magma (e.g., Bonin 1990; Patino Douce 1996; Rollinson 1993; Albaréde 1996).

The main problem to be solved for the A-type granites in the CACC is whether the distinctive trace-element characteristics of the intrusives can be related to mantle-source enrichment by recycling of crustal material (e.g., Gill 1981; Sun & McDonough 1989), or to fractional

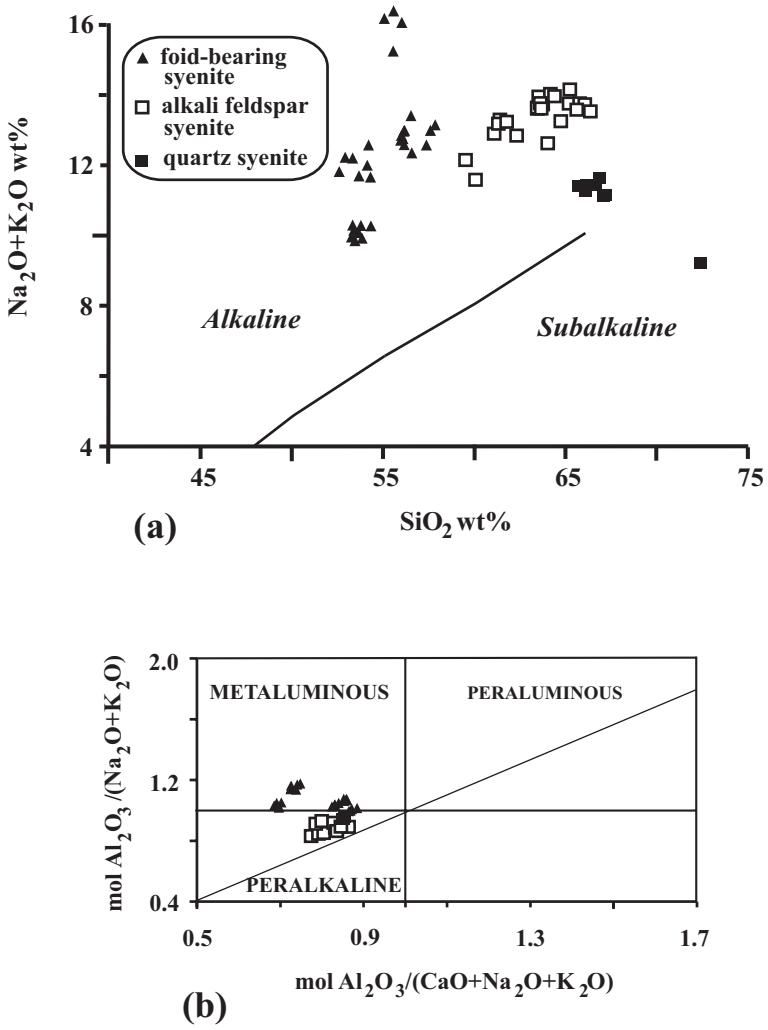

Figure 7. Classification of the intrusives: (a) total alkali versus silica diagram (after Irvine & Baragar 1971) showing alkaline character of the Hamit intrusives; (b) Shand's index values of the rock types (after Shand 1951).

crystallisation combined with crustal assimilation (AFC) (e.g., Hildreth & Moorbath 1988). Accordingly, the Th/Yb ratios of the plutonic rocks have been plotted against their Ta/Yb ratios (Figure 11). In Figure 11, a greywacke sample (N490: crust-C) (Table 3) from the Central Anatolian Crystalline Complex (CACC) is also plotted as the crustal contaminant. Figure 11 shows that all intrusive rocks from the pluton form trends that run parallel to the mantle metasomatism array but are displaced towards higher Th/Yb ratios, suggesting either derivation from an enriched mantle source to which a subduction component had been added, or coupled crustal contamination with fractional crystallisation, or both. As can be seen from Figure 11, the intrusive rocks do not form trends from the mantle array to the crust, so AFC is not likely the only process for the generation of these plutonic rocks.

The foid-bearing rocks in the Hamit pluton were probably derived from an undersaturated magma, and the alkali-feldspar/quartz syenites were also produced from this magma by means of extensive open-system AFC processes. Otlu (1998) and Otlu & Boztuğ (1998) also pointed out two rock groups in the CACC, but with a different genetic explanations; they suggested that these rocks were derived from two distinct alkaline magmas: (i) silica-oversaturated and (ii) silica-undersaturated.

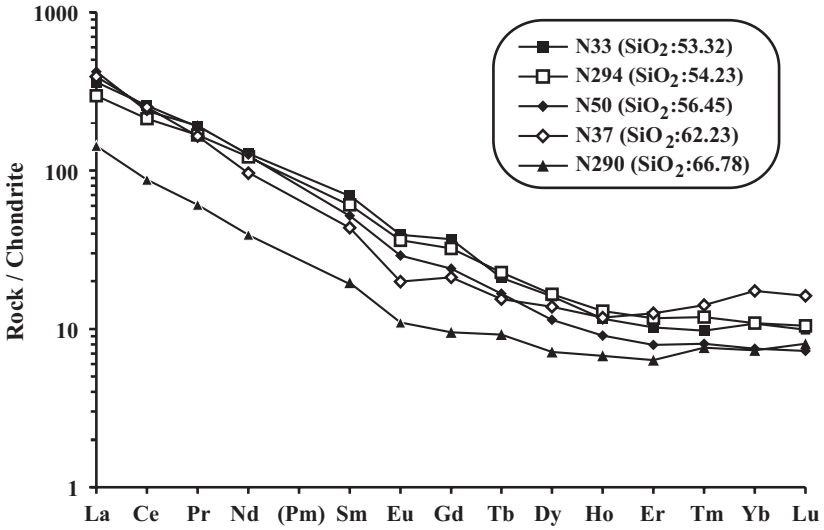

Figure 8. Chondrite-normalised REE patterns of the intrusive samples from the complex. Normalisation factors are taken from Boynton (1984).

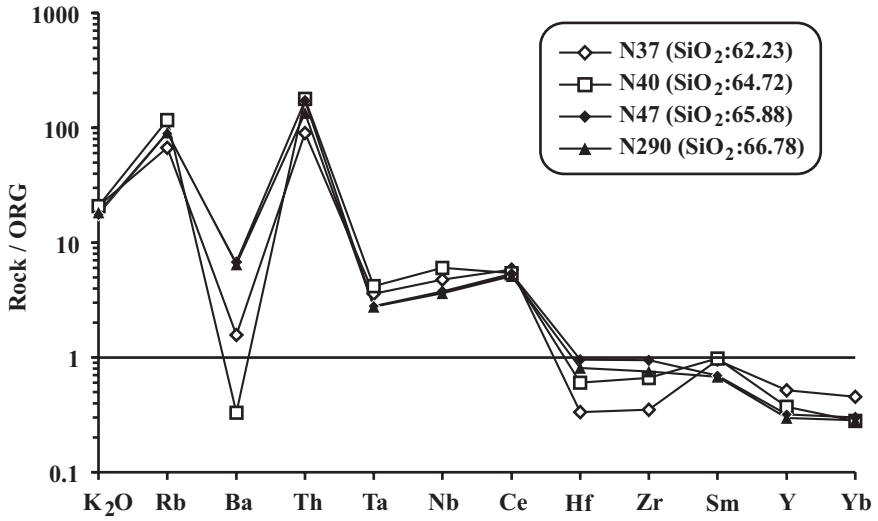

Figure 9. Ocean ridge granite (ORG) normalised diagram illustrating the geochemical characteristics of the intrusives (samples > 5% modal quartz are plotted) (normalising factors after Pearce *et al.* 1984).

For the case of central Anatolian intrusives, which have been shown to have been derived from a subduction-modified mantle source(s), the likely mechanisms for magma generation are: (i) lithospheric extension or uplift; or (ii) melting of mantle lithosphere by perturbation of the geotherm. The validity of the first mechanism depends mainly on the amount and the age of the initiation of extension. Although some authors (e.g., Gautier *et al.* 2002) suggest that localised extension affected the complex in Campanian (and possibly earlier) to Palaeocene times, more detailed radiometric data are needed to constrain the possibility of magmatism by lithospheric extension.

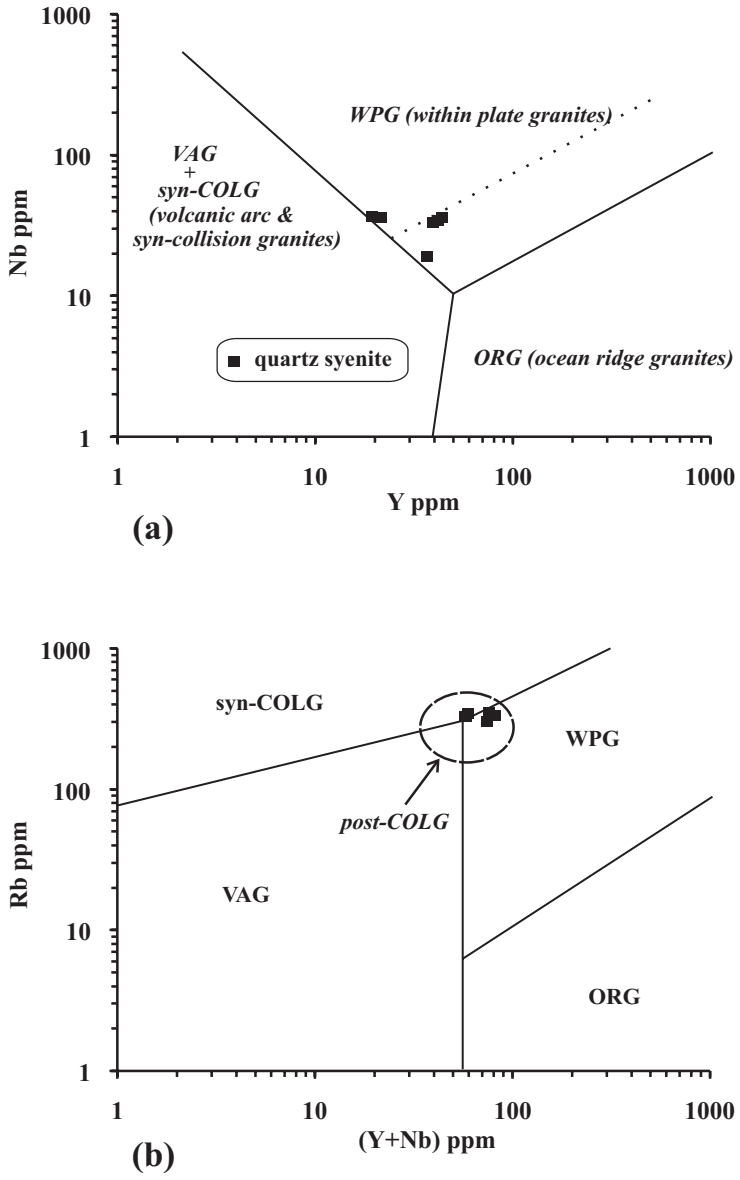

Figure 10. Tectonic discrimination diagrams of the intrusives (after Pearce *et al.* 1984) (samples > 5% modal quartz are plotted): (a) the Nb versus Y diagram; (b) the Rb versus (Y+Nb) diagram (after Pearce 1996).

Perturbation of subduction-metasomatised lithosphere by either delamination of the thermal boundary layer (TBL) or slab detachment may have generated the primary magmas of the alkaline Central Anatolian plutonic rocks (İlbeyli 1999; İlbeyli *et al.* 2004). Both processes would lead to conductive heating of enriched mantle, and this may have facilitated or initiated the orogenic collapse that followed collision and uplift. A similar mechanism has also been suggested for the origins of eastern and western Anatolian volcanic rocks (e.g., Pearce *et al.* 1990; Keskin 2003; Aldanmaz *et al.* 2000).

In summary, the intrusive rocks of the Hamit pluton in the CACC can be divided into two main groups on the basis of their petrographical-mineralogical and major- and trace- element characteristics; namely, (i) foid-bearing rocks and (ii) alkali-feldspar/quartz syenite. The Hamit intrusive rocks are alkaline in character. The peralkaline Hamit intrusive rocks (the alkali-feldspar syenite and

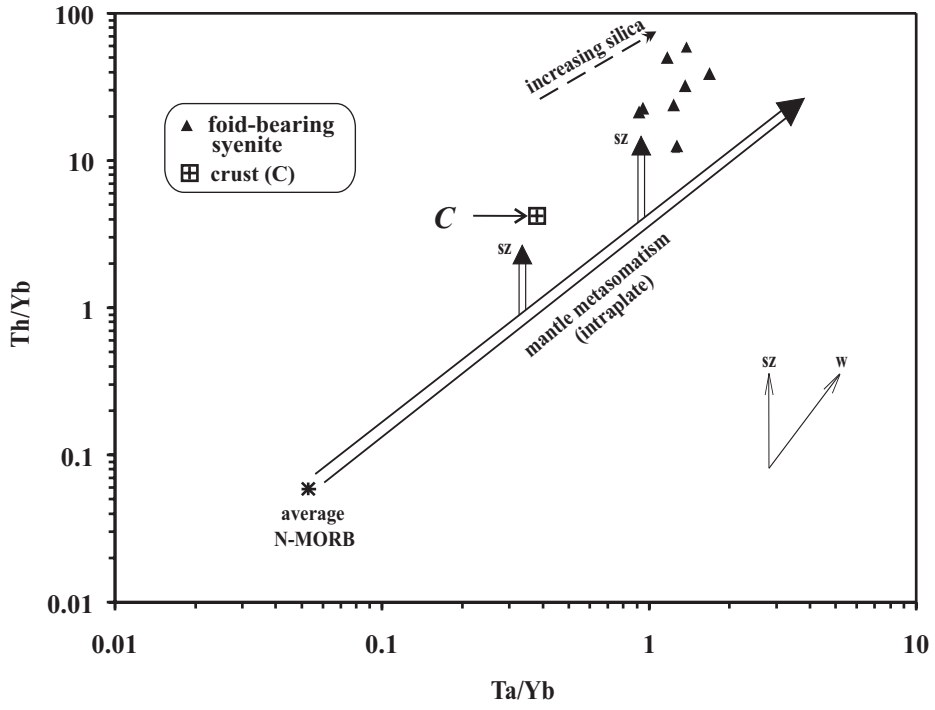

Figure 11. Th/Yb versus Ta/Yb diagram (after Pearce 1983) for basic and intermediate intrusive rocks (samples <63% SiO_2 are plotted) from the Hamit pluton. sz– subduction and w– within plate.

quartz syenite) have petrographic and geochemical characteristics similar to A-type granites. All Hamit intrusive rocks show enrichment in LILE (except Ba) and LREE relative to HFSE. The parental magmas for the Hamit intrusive rocks were generated from mantle sources which were modified by a subduction component before collision. These magmas have also experienced coupled crustal assimilation and fractional crystallisation (AFC) during ascent through the central Anatolian crust (İlbeyli 1999).

Acknowledgements

The author acknowledges Mustafa Kemal University for providing financial support during her studies. She also thanks Prof. Dr. Julian A. Pearce for his helpful comments and criticisms. Two anonymous reviewers are gratefully acknowledged for their comments on earlier versions of the manuscript that led to this improved final version.

References

Akıman, O., Erler, A., Göncüoğlu, M.C., Güleç, N., Geven, A., Türeli, K. & Kadıoğlu, Y.K. 1993. Geochemical characteristics of granitoids along the western margin of the Central Anatolian Crystalline Complex and their tectonic implications. *Geological Journal* **28**, 371–382.

Albaréde, F. 1996. *Introduction to Geochemical Modeling*. Cambridge University Press.

Aldanmaz, E., Pearce, J.A., Thirlwall, M.F. & Mitchell, J.G. 2000. Petrogenetic evolution of late Cenozoic, post-collision volcanism in western Anatolia, Turkey. *Journal of Volcanology and Geothermal Research* **102**, 67–95.

Ataman, G. 1972. A study on the radiometric age of Cefalıkdağ, one of the granite-granodiorite bodies outcropping on the south-east Ankara. *Yerbilimleri, Hacettepe University Science and Engineering Journal* **2**, 44–49 [in Turkish with English abstract].

AYDIN, N.S., GÖNCÜOĞLU, M.C. & ERLER, A. 1998. Latest Cretaceous magmatism in the Central Anatolian Crystalline Complex: brief review of field, petrographic and geochemical features. *Turkish Journal of Earth Sciences* **7**, 258–268.

AYDIN, N.S., MALPAS, J., GÖNCÜOĞLU, M.C. & ERLER, A. 2001. A review of the nature of magmatism in central Anatolia during the Mesozoic post-collisional period. *International Geology Review* **43**, 695–710.

BAYHAN, H. 1988. Geochemistry and genetic interpretation of alkaline rocks in the Bayındır-Akpınar (Kaman) area. *Geological Bulletin of Turkey* **31**, 59–69 [in Turkish with English abstract].

BAYHAN, H. & TOLLUOĞLU, A.Ü. 1987. The mineralogical-petrographical and geochemical characteristics of the Çayağazı syenitoid (northwest of Kırşehir province). *Bulletin of Earth Sciences Application and Research Centre of Hacettepe University* **14**, 109–120 [in Turkish with English abstract].

BİNGÖL, E. 1989. *Geological Map of Turkey*, *1:2,000,000*. Mineral Research and Exploration Institute of Turkey (MTA) Publications [in Turkish with English abstract].

BONIN, B. 1990. From orogenic to anorogenic settings: evolution of granitoid suites after a major orogenesis. *Geological Journal* **25**, 261–270.

BOYNTON, W.V. 1984. Geochemistry of the rare earth elements: meteorite studies. *In*: HENDERSON, P. (ed), *Rare Earth Element Geochemistry*, Elsevier, 63–114.

BOZTUĞ, D. 1998. Post-collisional central Anatolian alkaline plutonism. *Turkish Journal of Earth Sciences* **7**, 145–165.

BOZTUĞ, D. 2000. S-I-A type intrusive associations: geodynamic significance of synchronism between metamorphism and magmatism in central Anatolia, Turkey. *In*: BOZKURT, E., WINCHESTER, J.A. & PIPER, J.D. (eds), *Tectonics and Magmatism in Turkey and Surrounding Area*. Geological Society, London, Special Publications **173**, 441–458.

BOZTUĞ, D. YILMAZ, S. & KESGİN, Y. 1994. Petrography, petrochemistry and petrogenesis of the eastern part of Kösedağ pluton from the Central-Eastern Anatolian alkaline province, Suşehri, NE Sivas. *Geological Bulletin of Turkey* **32**, 1–12 [in Turkish with English abstract].

DALKILIÇ, F. 1986. *Petrography and Geochemistry of Felsic Intrusive Rocks from Northeast of Kaman Region (Kırşehir-Turkey)*. MSc Thesis, Middle East Technical University, Ankara-Turkey [unpublished].

DUCHESNE, J.C. 1984. Massif anorthosites: another partisan review. *In*: BROWN, W.L. (ed), *Feldspars and Feldspathoids: Structures, Properties and Occurences,* Kluwer Academic Publishers, 411–433.

DUCHESNE, J.C. 1990. Origin and evolution of monzonorites related to anorthosites. *Schweizerische Mineralogische und Petrographische Mitteilungen* **70**, 189–198.

EKİCİ, T., BOZTUĞ, D., TATAR, S. & OTLU, N. 1997. The co-existency of the syn-COLG and post-COLG granitoids in the Yozgat batholith from passive margin of the Anatolide-Pontide collision. *EUG 9 - Terra Nova Abstracts* **9**, p. 503.

EMSLIE, R.F. & STIRLING, J.A.R. 1993. Rapakivi and related granitoids of the Nain plutonic suite: geochemistry, mineral assemblages and fluid equilibria. *Canadian Mineralogist* **31**, 821–847.

ERLER, A., AKIMAN, O., UNAN, C., DALKILIÇ, B., GEVEN, A. & ÖNEN, P. 1991. Petrology and geochemisty of magmatic rocks around Kaman (Kırşehir) and Yozgat, Turkey. *Doğa, Turkish Journal of Engineering and Environmental Sciences* **15**, 76–100 [in Turkish with English abstract].

GAUTIER, P., BOZKURT, E., HALLOT, E. & DİRİK, K. 2002. Dating the exhumation of a metamorphic dome: geological evidence for pre-Eocene unroofing of the Niğde Massif (central Anatolia, Turkey). *Geological Magazine* **139**, 559–576.

GILL, J.B. 1981. *Orogenic Andesites and Plate Tectonics*. Springer-Verlag, Berlin.

GÖNCÜOĞLU, M.C. 1986. Geochronological data from the southern part (Niğde area) of the Central Anatolian Massif. *Mineral Research and Exploration Institute of Turkey (MTA) Bulletin* **105/106**, 111–124.

GÖNCÜOĞLU, M.C., TOPRAK, V., KUŞCU, İ., ERLER, A. & OLGUN, E. 1991. *Geology of the Western Part of the Central Anatolian Massif. Part I: Southern Section*. Turkish Petroleum Corporation (TPAO) Report No. **2909** [unpublished, in Turkish].

GÖNCÜOĞLU, M.C., ERLER, A., TOPRAK, V., OLGUN, E., YALINIZ, K.M., KUŞCU, İ., KÖKSAL, S. & DİRİK, K. 1993. *Geology of the Central Part of the Central Anatolian Massif. Part III: The Geological Evolution of the Kızılırmak Basin.* Turkish Petroleum Corporation (TPAO) Report No. **3313** [unpublished, in Turkish].

GÖNCÜOĞLU, M.C. KÖKSAL, S. & FLOYD, P.A. 1997. Post-collisional A-type magmatism in the Central Anatolian Crystalline Complex: petrology of the İdiş Dağı intrusives. *Turkish Journal of Earth Sciences* **6**, 65–76.

GÖRÜR, N. OKTAY, F.Y. SEYMEN, İ. & ŞENGÖR, A.M.C. 1984. Paleotectonic evolution of the Tuzgölü basin complex, central Anatolia (Turkey): sedimentary record of a Neo-Tethyan closure. *In*: DIXON, J.E. & ROBERTSON, A.H.F. (eds), *The Geological Evolution of the Eastern Mediterranean.* Geological Society, London, Special Publications **17**, 467–482.

GÜLEÇ, N. 1994. Rb-Sr isotope data from the Ağaçören granitoid (east of Tuz Gölü): geochronological and genetical implications. *Turkish Journal of Earth Sciences* **3**, 39–43.

GÜNDOĞDU, N., BROS, R., KURUÇ, A. & BAYHAN, H. 1988. Rb-Sr isotope data from the Bayındır feldspatoid-bearing syenites (Kaman-Kırşehir). *Twentieth Earth Sciences of Hacettepe University Symposium, Abstracts*, p. 55.

HILDRETH, W. & MOORBATH, S. 1988. Crustal contribution to arc magmatism in the Andes of southern Chile. *Contributions to Mineralogy and Petrology* **98**, 455–489.

HUPPERT, H.E. & SPARKS, R.S.J. 1988. The generation of granitic magmas by intrusion of basalt into continental crust. *Journal of Petrology* **29**, 569–624.

İLBEYLİ, N. 1999. *Petrogenesis of Collision-related Plutonic Rocks, central Anatolia (Turkey)*. PhD Thesis, University of Durham, Durham, UK [unpublished].

İLBEYLİ, N., PEARCE, J.A., THIRLWALL, M.F. & MITCHELL, J.G. 2004. Petrogenesis of collision-related plutonics in central Anatolia, Turkey. *Lithos* **72**, 163–182.

IRVINE, T.N. & BARAGAR, W.R.A. 1971. A guide to the chemical classification of the common volcanic rocks. *Canadian Journal of Earth Sciences* **8**, 523–548.

KADIOĞLU, Y.K., DİLEK, Y., GÜLEÇ, N. & FOLAND, K.A. 2003. Tectonomagmatic evolution of bimodal plutons in the Central Anatolian Crystalline Complex, Turkey. *The Journal of Geology* **111**, 671–690.

KESKİN, M. 2003. Magma generation by slab steepening and breakoff beneath a subduction-accretion complex: an alternative model for collision-related volcanism in eastern Anatolia, Turkey. *Geophysical Research Letters* **30**, 9/1–9/4.

KÖKSAL, S. GÖNCÜOĞLU, M.C. & FLOYD, P.A. 2001. Extrusive members of post collisional A-type magmatism in central Anatolia: Karahıdır Volcanics, İdiş Dağı-Avanos area, Turkey. *International Geology Review* **43**, 683–694.

KURUÇ, A. 1990. *Rb/Sr Geochemistry of Syenitoids from Kaman-Kırşehir Region.* MSc Thesis, Hacettepe University, Ankara, Turkey [unpublished].

LÜNEL, A.T. & AKIMAN, O. 1986. Pseudoleucite from Hamitköy area, Kaman, Kırşehir occurrence and its use as a pressure indicator. *Mineral Research and Exploration Institute of Turkey (MTA) Bulletin* **103/104**, 117–123 120 [in Turkish with English abstract].

OKAY, A.İ. TANSEL, İ. & TÜYSÜZ, O. 2001. Obduction, subduction and collision as reflected in the Upper Cretaceous-Lower Eocene sedimentary record of western Turkey. *Geological Magazine* **138**, 117–142.

OTLU, N. 1998. *A Petrological Investigation of the Plutonic Rocks Between the Kortundağ and Baranadağ Area (E Kaman, NW Kırşehir)*. PhD Thesis, Cumhuriyet University, Sivas-Turkey [unpublished; in Turkish with English abstract].

OTLU, N. & BOZTUĞ, D. 1998. The coexistence of the silica oversaturated (ALKOS) and undersaturated alkaline (ALKUS) rocks in the Kortundağ and Baranadağ plutons from the central Anatolian alkaline plutonism, E Kaman/NW Kırşehir, Turkey. *Turkish Journal of Earth Sciences* **7**, 241–257.

ÖZKAN, H.M. 1987. *Petrographical and Geochemical Investigation of Hayriye (Kayseri) Nepheline-Syenite Intrusion*. MSc thesis, Ankara University, Ankara-Turkey [unpublished; in Turkish with English abstract].

ÖZKAN, H.M. & ERKAN, Y. 1994. A petrological study on a foid syenite intrusion in central Anatolia (Kayseri-Turkey). *Turkish Journal of Earth Sciences* **3**, 45–55.

PATINO DOUCE, A.E. 1996. Effects of pressure and H_2O content on the compositions of primary crustal melts. *Transactions of the Royal Society of Edinburgh: Earth Sciences* **87**, 11–21.

PEARCE, J.A. 1983. Role of the sub-continental lithosphere in magma genesis at active continental margins. *In*: HAWKESWORTH, C.J. & NORRY, M.J. (eds), *Continental Basalts and Mantle Xenoliths*, Shiva Publications, 230–249.

PEARCE, J.A. 1996. Sources and settings of granitic rocks. *Episodes* **19**, 120–125.

PEARCE, J.A., HARRIS, N.B.W. & TINDLE, A.G. 1984. Trace element discrimination diagrams for the tectonic interpretation of granitic rocks. *Journal of Petrology* **25**, 956–983.

PEARCE, J.A., BENDER, J.F., DE LONG, S.E., KIDD, W.S.F., LOW, P.J. GÜNER, Y., ŞAROĞLU, F., YILMAZ, Y., MOORBATH, S. & MITCHELL, J.G. 1990. Genesis of collision volcanism in eastern Anatolia, Turkey. *Journal of Volcanology and Geothermal Research* **44**, 189–229.

PEATE, D.W., PEARCE, J.A., HAWKESWORTH, C.J., COLLEY, H., EDWARDS, C.M.H. & HIROSE, K. 1997. Geochemical variations in Vanuatu arc lavas: the role of subducted material and a variable mantle wedge composition. *Journal of Petrology* **38**, 1331–1358.

ROLLINSON, H.R. 1993. *Using Geochemical Data: Evaluation, Presentation, Interpretation*. John Wiley & Sons-USA.

ŞENGÖR, A.M.C. & YILMAZ, Y. 1981. Tethyan evolution of Turkey: a plate tectonic approach. *Tectonophysics* **75**, 181–241.

SEYMEN, İ. 1981. Metamorphism of the Kırşehir Massif around Kaman (Kırşehir). *Symposium on Geology of Central Anatolia*. Turkish Geological Society, Special Publications, 12–15.

SEYMEN, İ. 1982. *Geology of the Kırşehir Massif around Kaman*. DSc Thesis, İstanbul Technical University, İstanbul, Turkey [unpublished; in Turkish with English abstract].

SEYMEN, İ. 1985. Geological evolution of the Kırşehir Massif metamorphics. *Proceedings of Ketin Symposium*. Turkish Geological Society, Special Publications, 133–148.

SHAND, S.J. 1951. *Eruptive Rocks*. John Wiley, New York, USA.

STRECKEISEN, A. 1976. To each plutonic rock its proper name. *Earth-Science Reviews* **12**, 1–33.

SUN, S.S. & MCDONOUGH, W.F. 1989. Chemical and isotopic systematics of oceanic basalts: implications for mantle composition and processes. *In*: SAUNDERS, A.D. & NORRY, M.J. (eds), *Magmatism in the Ocean Basins*. Geological Society, London, Special Publications **42**, 313–345.

TOLLUOĞLU, A.Ü. 1993. The petrographical and geochemical characteristics of felsic intrusives (Kötüdağ and Buzlukdağ) cutting Kırşehir Massif. *Bulletin of Earth Sciences Application and Research Centre of Hacettepe University* **16**, 19–41 [in Turkish with English abstract].

TURNER, S.P., FODEN, J.D., DEBLOND, A. & DUCHESNE, J.C. 1992. Derivation of some A-type magmas by fractionation of basaltic magma: an example from the Padhaway Ridge, South Australia. *Lithos* **28**, 23–55.

TÜYSÜZ, O., DELLALOĞLU, A.A. & TERZİOĞLU, N. 1995. A magmatic belt within the Neo-Tethyan suture zone and its role in the tectonic evolution of northern Turkey. *Tectonophysics* **243**, 17–191.

YALINIZ, K.M., AYDIN, N.S., GÖNCÜOĞLU, M.C. & PARLAK, O. 1998. Terlemez quartz monzonite of central Anatolia (Aksaray-Sarıkaraman): age, petrogenesis and geotectonic implications for ophiolite emplacement. *Third International Turkish Geology Symposium, Abstracts*, p. 161.

ZECK, H.P. & ÜNLÜ, T. 1987. Parallel whole-rock isochrons from a composite, monzonitic pluton, Alpine belt, central Anatolia, Turkey. *Neues Jahrbuch fur Mineralogie, Abhandlungen* **5**, 193–204.

Received 22 October 2003; revised typescript accepted 18 August 2004